Theor Chem Acc (2002) 107:266–271
DOI 10.1007/s00214-002-0323-4

Theoretical
Chemistry Accounts

Regular article

Density functional theory gas- and solution-phase study of nucleophilic substitution at di- and trisulfides

Steven M. Bachrach, Joseph M. Hayes, Trang Dao, Justin L. Mynar

Department of Chemistry, Trinity University, 715 Stadium Drive, San Antonio, TX 78212, USA

Received: 12 October 2001 / Accepted: 28 November 2001 / Published online: 8 April 2002

Abstract. Density functional calculations indicate that nucleophilic substitution in the thiolate–disulfide and thiolate–trisulfide exchange reactions proceeds by an addition–elimination pathway. Solution calculations were performed using B3LYP/6-31 + G* and the polarized continuum method. These solution-phase calculations indicate that for the reactions where the sulfur under attack bears a hydrogen atom, the substitution proceeds via an addition–elimination mechanism; however, when a methyl group is attached to the sulfur under attack, the S_N2 mechanism is predicted.

Key words: Nucleophilic substitution – Disulfide – Trisulfide – DFT – Solvent effects

1 Introduction

The study of nucleophilic substitution provides an important paradigm for analysis of reaction mechanisms [1]. While the majority of studies have concentrated on substitution at carbon, substitution reactions at heteroatoms are interesting both from synthetic and mechanistic viewpoints. Of interest here is nucleophilic substitution at sulfur, which plays important roles in many biochemical processes, such as affecting protein structure through attack at the disulfide bridge [2, 3] and the activation of many ene–diyne antitumor agents [4]. Experimental studies have concentrated on substitution of disulfides in solution [5, 6, 7, 8, 9]. Kinetics studies show bimolecularity, solvent dependencies, Brönsted β_{nuc} and entropy values that are consistent with an S_N2 mechanism.

Bachrach and Mulhearn reported ab initio calculations of nucleophilic substitution at sulfur for both the thiolate–disulfide exchange [10] and the thiolate–trisulfide exchange [11]. Among the reactions they examined are the six listed in Scheme 1. Hartree–Fock (HF) calculations predict a classic gas-phase S_N2 mechanism in all these cases; however, MP2/6-31 + G* and MP4/6-31 + G*//MP2/6-31 + G* calculations find an addition–elimination mechanism. The HF transition state (TS) becomes a local energy minimum (an intermediate on the reaction coordinate) when electron correlation is included; however, the depth of this intermediate well is shallow. The well depth is 2.2–2.4 kcalmol^{-1} for reactions 1 and 2 at either MP2 or MP4; it is only 0.1 kcal mol^{-1} for reaction 3 at MP2 and disappears at MP4. Similar shallow wells are seen for the trisulfides. We have recently shown that the intermediate can, in fact, be greatly stabilized; for the reactions of chloride with SCl_2 and $SOCl_2$, the minimum on the potential-energy surface (PES) is the species where the nucleophile has added to the sulfur, i.e., SCl_3^- and $SOCl_3^-$, respectively [12, 13]. Gas-phase flow–afterglow mass spectrometry studies identified these two species and corroborate the depth of the computed well. Additionally, in the case of the trisulfides, where attack can occur at a terminal or a central sulfur, the barrier for terminal attack is preferred by 2–5 kcal mol^{-1} [11].

In this work, we address (in part) two questions concerning nucleophilic substitution at sulfur. First, we further explore the computational dependency on the nature of the PES. In addition to the previously reported MP2, MP4 and CCSD studies [10, 11], we report here density functional theory (DFT) calculations that wholly support the addition–elimination pathway. Second, while all the computational work so far represents the gas phase, the experiments are principally solution-phase. We report here polarized continuum model

Scheme 1. Di- and trisulfide reactions

Disulfide reactions	
$HS^- + HSSH \rightarrow HSSH + HS^-$	Reaction 1
$CH_3S^- + HSSCH_3 \rightarrow CH_3SSH + CH_3S^-$	Reaction 2
$HS^- + CH_3SSH \rightarrow HSSCH_3 + HS^-$	Reaction 3
Trisulfide reactions	
$HS^- + HSSSH \rightarrow HSSSH + HS^-$	Reaction 4
$HS^- + HSSSH \rightarrow HSSH + HSS^-$	Reaction 5
$HS^- + CH_3SSSH \rightarrow HSSCH_3 + HSS^-$	Reaction 6

Correspondence to: S.M. Bachrach

(PCM) calculations as a first attempt to model nucleophilic substitution at sulfur in solution.

2 Computational method

Reactions 1–6 shown in Scheme 1 model nucleophilic substitution at sulfur in di- and trisulfides. Reactions 1 and 2 compare the effect of methyl substitution on the action of the nucleophile, while reactions 1 and 3 compare the effect of methyl (steric) substitution upon the sulfur under attack. Reactions 4 and 5 compare attack at the central versus the terminal sulfur of the trisulfide. Reactions 5 and 6 again compare the effect of methyl substitution upon the sulfur under attack. All the computations were performed using the GAUSSIAN 98 package [14].

The first part of the study is to compare various DFT models for the gas-phase thiolate–disulfide exchange with our previous studies at MP2 and MP4. Reactions 1–3 were examined at the B3LYP/6-31 + G*, B3LYP/aug-cc-pVTZ and BPW91/aug-cc-pVTZ levels in order to compare the geometries and energetics [15–19]. On the basis of the results of these computations, the B3LYP/6-31 + G* level was deemed sufficiently accurate for our purposes, and this method was hence used solely to study the gas-phase trisulfide exchange (reactions 4–6) and the solvation model studies of the complete set of reactions 1–6.

For the solution-phase studies, solvation was modeled via the PCM as implemented in GAUSSIAN 98 [20, 21, 22]. This is a simple continuum model and has been successfully applied to related systems [23, 24, 25, 26]. The default uniform dielectric constant of 78.39 for water was used in all the calculations. Initial attempts to model solvation using the GAUSSIAN 98 default PCM parameters provided nonsensical results, such as TSs lower in energy than the intermediates. Close analysis revealed the problem lay with the assignment of the atomic cavities. GAUSSIAN 98 uses the united atom model for HF (UAHF) method for calculation of atomic sphere radii from which the solute cavity is built [27]. The UAHF model builds the cavity according to properties such as the molecular topology, hybridization and formal charge. In the charged species involved in reactions 1–6, the default procedure is to allocate the charge on an equal basis to all heavy atoms. This assignment is radically different from the charge distribution assigned by either the Mulliken or the natural population analyses [28]. Therefore, cavity sizes were obtained using Eq. (1), proposed by Barone et al. [27] for ions. The atomic radii of spheres, $R(X)$, where X is the atom, depends on the atomic radius for the neutral species, $R^0(X)$, and the charge, q, which we take as the atomic Mulliken charge determined in the optimum gas-phase structure. We used this procedure for calculation of the atomic sphere radii of all heavy atoms in our systems; a correction factor, α, of −0.3 was used for all atoms bearing negative Mulliken charges and a correction factor of −0.55 was used for atoms bearing positive Mulliken charges. Free energies are reported for the solution-phase calculations, evaluated at 298 K with no scaling for the zero-point energy (ZPE).

$$R(X) = R^0(X) + \alpha_q|q| \quad (1)$$

To characterize the stationary points and obtain ZPE for both the gas- and the solution-phase studies, computation of analytical frequencies was performed for all optimum geometries. The minima are characterized by having all-real frequencies, while the presence of one imaginary frequency (with the correct imaginary mode) characterizes the TSs. All energies were corrected with scaled ZPE; the ZPE scaling factors of 0.96, 0.98 and 0.98 were used for the B3LYP/6-31 + G(d), B3LYP/aug-cc-pVTZ and B3PW91/aug-cc-pVTZ energies, respectively [29, 30].

3 Results and discussion

3.1 DFT studies

Gas-phase nucleophilic substitution reactions are characterized by the presence of ion–dipole complexes that precede the actual substitution reaction. A sketch of the PES for a generic gas-phase S_N2 reaction is shown in Fig. 1a. This double-well PES is found for the thiolate–disulfide exchange at the HF level; however, we found that the surface has three wells (Fig. 1b) at the MP2 level, indicating an addition–elimination mechanism. Our goal in this section is to determine the nature of the PES when various DFT methods are employed.

The results of the DFT studies for reactions 1–3 are shown in Tables 1 and 2. The important geometric parameters for the intermediates and the TSs in reactions 1–3 are listed in Table 1, while their relative energies are listed in Table 2. Drawings of the TSs and the intermediates are shown in Fig. 2. The existence of the ion–dipole complexes is assumed here, since our interest lies principally with characterization of the reaction mechanism. We employed three different DFT methods: two different functionals (B3LYP and B3PW91) and two different basis sets (6-31 + G* and aug-cc-pVTZ). Comparison is made to the previous MP2/6-31 + G* results [10].

All three DFT methods provide PES of the same shape for all three reactions. Each reaction is characterized by two TSs surrounding a stable intermediate, indicative of an addition–elimination pathway.

Reactions 1 and 2 represent nucleophilic attack at an unsubstituted sulfur. The DFT TSs for these two reactions are similar. The S_{nuc}–S distance is about 3.2 Å and the S–S_{lg} distance is about 2.2 Å, while the putative hydrogen bond between the formal sulfur anion and hydrogen is about 2.4 Å. The angle between the three sulfur atoms is about 147° in TS-1 and 150° in TS-2. The B3PW91 distances are all slightly shorter than the B3LYP values. The DFT results differ from the MP2 results in the hydrogen-bond length and the angle about the sulfur, due most likely to DFT predicting a stronger hydrogen bond than MP2.

The intermediates of reactions 1 and 2 possess slightly nonlinear S–S–S angles with nearly equal S–S distances. This is found for all the computations (DFT and MP2)

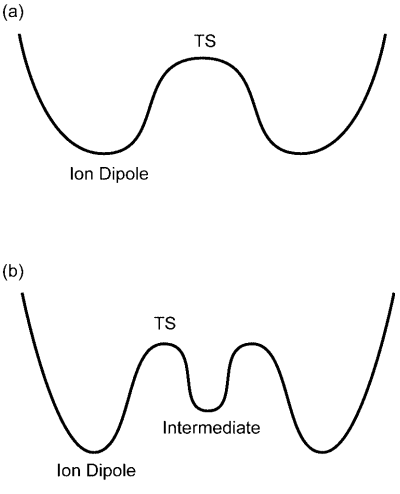

Fig. 1. Schematic of the potential-energy surfaces for the gas-phase **a** S_N2 and **b** addition–elimination mechanisms, showing the transition states (TSs)

Table 1. Selected distances (Å) and angles (degrees) for intermediates and transition states (*TSs*) in reactions 1–3 calculated in the gas phase. See Fig. 2 for definitions

Compound	Level	S_{nuc}–S	S–S_{lg}	*R*S···H	S_{nuc}–S–S_{lg}
TS-1	B3LYP/6-31 + G*	3.238	2.185	2.427	146.0
	B3LYP/aug-cc-pVTZ	3.213	2.159	2.406	146.3
	B3PW91/aug-cc-pVTZ	3.134	2.125	2.365	147.9
	MP2/6-31 + G*	3.186	2.123	2.621	153.7
INT-1	B3LYP/6-31 + G*	2.512	2.510	–	173.5
	B3LYP/aug-cc-pVTZ	2.485	2.486	–	172.8
	B3PW91/aug-cc-pVTZ	2.436	2.435	–	172.2
	MP2/6-31 + G*	2.467	2.467	–	174.4
TS-2	B3LYP/6-31 + G*	3.173	2.177	2.432	149.1
	B3LYP/aug-cc-pVTZ	3.147	2.152	2.407	149.3
	B3PW91/aug-cc-pVTZ	3.062	2.119	2.354	150.6
	MP2/6-31 + G*	3.089	2.118	2.573	155.7
INT-2	B3LYP/6-31 + G*	2.498	2.496	–	173.9
	B3LYP/aug-cc-pVTZ	2.470	2.469	–	173.1
	B3PW91/aug-cc-pVTZ	2.419	2.417	–	172.6
	MP2/6-31 + G*	2.450	2.449	–	172.4
TS-3	B3LYP/6-31 + G*	4.004	2.114	2.580	166.9
	B3LYP/aug-cc-pVTZ	3.955	2.107	2.562	168.1
	B3PW91/aug-cc-pVTZ	3.838	2.078	2.501	169.1
	MP2/6-31 + G*	2.813	2.232	2.700	177.1
INT-3	B3LYP/6-31 + G*	2.562	2.491	–	175.3
	B3LYP/aug-cc-pVTZ	2.562	2.447	–	175.5
	B3PW91/aug-cc-pVTZ	2.517	2.389	–	176.7
	MP2/6-31 + G*	2.480	2.469	–	177.8

Table 2. Gas-phase relative energies (kcalmol^{-1}) for reactions 1–3. The well depth is defined as *E*(TS)−*E*(INT)

Level	Reactants	TS	INT	Well depth
Reaction 1				
B3LYP/6-31 + G*	0.0	−13.3	−18.4	5.1
B3LYP/aug-cc-pVTZ	0.0	−12.9	−17.0	4.1
B3PW91/aug-cc-pVTZ	0.0	−13.4	−17.4	4.0
MP2/6-31 + G*	0.0	−10.7	−12.9	2.2
Reaction 2				
B3LYP/6-31 + G*	0.0	−12.7	−16.9	4.2
B3LYP/aug-cc-pVTZ	0.0	−11.9	−15.4	3.5
B3PW91/aug-cc-pVTZ	0.0	−12.9	−16.3	3.4
MP2/6-31 + G*	0.0	−11.3	−13.8	2.5
Reaction 3				
B3LYP/6-31 + G*	0.0	−7.7	−12.2	4.5
B3LYP/aug-cc-pVTZ	0.0	−7.9	−10.7	2.8
B3PW91/aug-cc-pVTZ	0.0	−8.4	−11.1	2.7
MP2/6-31 + G*	0.0	−8.3	−8.4	0.1

with little variation in S–S distances or S–S–S angle with computational method or even between INT-1 and INT-2.

The energetics of reactions 1 and 2 are listed in Table 2. These reactions define a triple-well PES, and the key characteristic is the depth of the central well, defined as the energy difference between the TS and the intermediate (called ''well depth'' in Table 1). The DFT PESs are very similar, differing by no more than 1 kcalmol^{-1}. These intermediates lie below the reactants, and in wells of 3–5 kcalmol^{-1}. The MP2 surface is topologically identical, though the TSs and the intermediates are more stabilized relative to reactants at DFT than at MP2. Further, the wells defining the intermediates are deeper at DFT than MP2 by a couple of kilocalories per mole.

The nucleophile attacks a methyl-substituted sulfur in reaction 3. The DFT TSs again are very similar, and except for a much longer S–S_{nuc} distance, resemble the TSs of reactions 1 and 2. The longer S–S_{nuc} distance comes from the hydrogen bond belonging to a methyl hydrogen instead of to a sulfur hydrogen. Most notably, however, is the dramatic difference between the structure of the DFT TSs and the MP2 TS. The S_{nuc}–S distance is a full angstrom shorter and the S–S_{lg} distance is 0.1–0.2 Å longer at MP2 than at DFT, indicating that the MP2 TS is substantially later than the DFT TSs.

DFT predicts that the two S–S distances are not quite as similar in INT-3 as in the other two intermediates, but the S–S–S angle is close to linearity. These DFT intermediates are also not symmetric, as predicted by MP2 for INT-3.

Again, all the methods indicate that reaction 3 proceeds via a triple-well, indicative of an addition–elimination reaction. Consistent with the very late MP2 TS, MP2 predicts a very small well depth for the intermediate, though the DFT methods predict a deeper well of 2.7–4.5 kcal mol^{-1}.

A number of conclusions can be drawn at this stage. The DFT methods are very consistent in terms of the structures of the intermediates and the TSs. The key feature of the PES is the existence of the intermediate and the depth of the well it resides in. All the methods agree that the three reactions proceed by a triple-well addition–elimination process in the gas phase. The well depth is greater at DFT than at MP2. There is a basis-set dependence, with the smaller basis set (6-31 + G*) giving a deeper well than the larger basis set (aug-cc-pVTZ), though this difference is always less that 2 kcal mol^{-1} and is usually less than 1 kcalmol^{-1}. There is little difference between the B3LYP and B3PW91 functionals; therefore, we

utilized the B3LYP/6-31 + G* method for the examination of solvation effects as a balance of accuracy against speed of computation.

We examined the prototype thiolate–trisulfide exchanges represented in reactions 4–6 at the B3LYP/6-31 + G* level and compared these results with our previous MP2/6-31 + G* calculations [11]. The structures of the TSs and the intermediates are drawn in Fig. 2, key geometric parameters are listed in Table 3 and their relative energies are reported in Table 4.

Reactions 4 and 5 differ in which site of the trisulfide undergoes the nucleophilic attack: the central sulfur (reaction 4) or a terminal sulfur (reaction 5). For both reactions, an intermediate is located along with entrance and exit TSs using both MP2 and B3LYP. The B3LYP and MP2 structures of TS-4 are quite different; the MP2

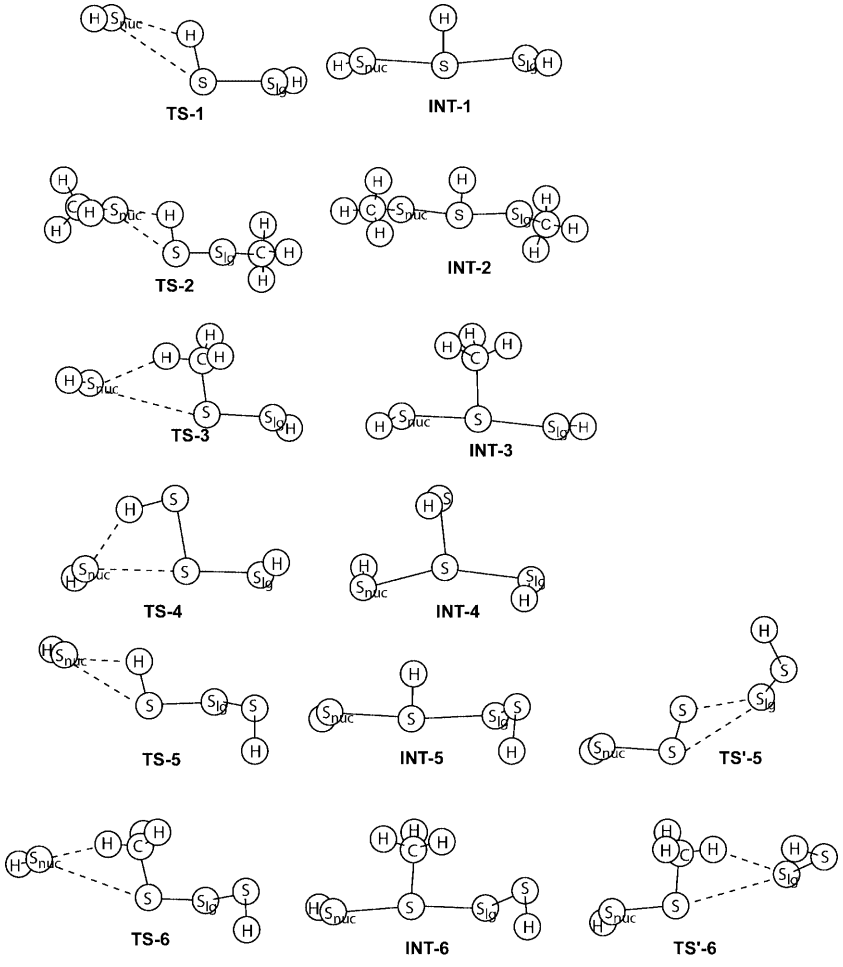

Fig. 2. Optimized gas-phase geometries of the TSs and the intermediates for reactions 1–6

Table 3. Selected distances (Å) and angles (degrees) for intermediates and TSs in reactions 4–6 calculated in the gas phase. See Fig. 2 for definitions

	Level	S_{nuc}–S	S–S_{lg}	HS···S	S_{nuc}–S–S_{lg}
TS-4	B3LYP/6-31 + G*	3.082	2.188	2.260	179.3
	MP2/6-31 + G*	2.620	2.340	2.793	173.9
INT-4	B3LYP/6-31 + G*	2.535	2.539	–	157.6
	MP2/6-31 + G*	2.513	2.472	–	163.0
TS-5	B3LYP/6-31 + G*	3.198	2.146	2.415	147.6
	MP2/6-31 + G*	3.187	2.093	2.560	152.1
INT-5	B3LYP/6-31 + G*	2.503	2.485	–	173.7
	MP2/6-31 + G*	2.448	2.445	–	173.2
TS′-5	B3LYP/6-31 + G*	2.175	3.288	2.465	145.1
	MP2/6-31 + G*	2.087	3.556	2.682	139.7
TS-6	B3LYP/6-31 + G*	4.166	2.083	2.536	162.9
	MP2/6-31 + G*	3.779	2.057	2.525	169.6
INT-6	B3LYP/6-31 + G*	2.534	2.472	–	172.5
	MP2/6-31 + G*	2.458	2.441	–	175.3
TS′6	B3LYP/6-31 + G*	2.129	3.926	2.586	168.3
	MP2/6-31 + G*	2.083	3.679	2.581	170.6

Table 4. Gas-phase relative energies (kcalmol^{-1}) for reactions 1–3. The well depth is that of the forward direction

Level	Reactants	TS	INT	TS′	Products	Well depth
Reaction 4						
B3LYP/6-31+G*	0.0	−12.2	−14.1	−12.2	0.0	1.9
MP2/6-31+G*	0.0	−9.6	−10.3	−9.6	0.0	0.7
Reaction 5						
B3LYP/6-31+G*	0.0	−15.2	−19.5	−13.6	−1.9	4.3
MP2/6-31+G*	0.0	−12.7	−15.1	−13.2	−1.6	2.4
Reaction 6						
B3LYP/6-31+G*	0.0	−9.4	−13.4	−7.8	−6.5	4.0
MP2/6-31+G*	0.0	−10.1	−10.8	−9.7	−0.3	0.7

TS is much later than the B3LYP. However, both methods predict very similar structures for INT-4. B3LYP predicts a more stable intermediate sitting in a deeper well than that predicted by MP2. On the other hand, both methods predict similar geometries for TS-5 and INT-5. TS-5 is similar to TS-1 in the parameters that are involved in the reaction (those listed in the tables). As for reaction 1, B3LYP predicts a more stable intermediate in a deeper well for reaction 5.

Reaction 6 involves nucleophilic attack at a terminal sulfur, now having a methyl substituent. This allows comparison to reaction 3, which also involves attack at a methyl-substituted sulfur. Again, a triple-well PES is found at both B3LYP and MP2. In reaction 3, MP2 gave a much later TS than B3LYP; here in reaction 6, this ordering is true, but the MP2 TS is later only in the extent of the creation of the new S–S bond – the other geometric parameters are quite similar. Both methods provide nearly identical structures of the intermediate. Consistent with all the other reactions, B3LYP predicts a more stable intermediate in a deeper well than MP2. The well depth for INT-6 is only slightly less (0.3 kcal mol^{-1}) than for INT-5 at B3LYP, and is very different from the MP2 result (1.7 kcal mol^{-1}). This same trend is also seen in the comparison of Reactions 1 and 3.

We [11] had previously commented on the preference for terminal over central attack in the trsiulfide [31]. This kinetic preference is confirmed with these B3LYP calculations, with the difference in barrier heights for the two processes (reaction 4 versu. 5) being nearly identical at MP2 and B3LYP.

In summary, the gas-phase examination of reactions 1–6 shows a consistent picture. Nucleophilic substitution at sulfur in di- and trisulfides proceeds by an addition–elimination process. B3LYP predicts a deeper well for the intermediates of these reactions. While methyl substitution at the site of attack decreases the well depth at MP2, this reduction is attenuated at B3LYP.

3.2 Solution-phase studies

We employed the PCM as an initial attempt to account for the effect of solvation in nucleophilic substitution at sulfur. As described in the Section 2, it was necessary to alter the atomic radius of the heavy atoms to account for the charge distribution in the TSs and the intermediates.

Table 5. Selected distances (Å) and angles (degrees) for intermediates and TSs in reactions 1–6 calculated in the solution (water) phase

Stucture	S_{nuc}–S	S–S_{lg}	HS···S	S_{nuc}–S–S_{lg}
TS-1	3.111	2.121	2.467	141.8
INT-1	2.496	2.464	–	175.9
TS-2	3.298	2.120	2.454	145.9
INT-2	2.477	2.463	–	175.5
TS-3	2.524	2.470	–	174.4
TS-4	2.879	2.217	2.497	177.0
INT-4	2.515	2.514	–	158.3
TS-5	3.233	2.114	2.539	149.6
INT-5	2.353	2.580	–	175.3
TS′-5	2.118	3.346	2.729	149.3
TS-6	2.510	2.471	–	177.2

Table 6. Solution- (water) phase relative free energies (kcal mol^{-1}) for reactions 1–6

Reaction	Reactants	TS	INT or TS	TS′	Products
1	0.0	7.8	4.5 (INT)	7.8	0.0
2	0.0	6.0	3.7 (INT)	6.0	0.0
3	0.0		10.9 (TS)		0.0
4	0.0	13.9	11.7 (INT)	13.9	0.0
5	0.0	9.2	6.9 (INT)	10.7	7.8
6	0.0		14.2 (TS)		−8.5

With this procedure, we optimized the structures involved in reactions 1–6 at B3LYP/6-31+G* including the PCM. The solvent was taken to be water. The critical geometric parameters are listed in Table 5. Since the PCM is parameterized to produce ΔG, the relative Gibbs free energies are reported in Table 6.

Our main interest here is the nature of the reaction mechanism or, in other words, the presence or absence of an intermediate on the PES. Therefore, we did not search for any ion–dipole intermediates, though there is precedence that these structures do not persist in the aqueous phase [32].

For reactions 1, 2, 4 and 5 solvent affects the energetics and geometries but not the mechanism. The solvent effect on the molecular geometries is fairly small. The solution- and gas-phase S–S distances differ by less than 0.15 Å for the intermediates and by no more than 0.2 Å for the TSs. TS-4 is significantly later than the other TSs in the solution phase. This is consistent with

the Hammond postulate, as formation of the intermediate of reaction 4 is more endothermic than for these others. This probably arises from a combination of steric hindrance and entropic differences attributable to comparing attack at a terminal sulfur (reactions 1, 2 and 5) versus attack at a central sulfur (reaction 4).

It is not possible to directly compare the free energies determined in solution (Table 6) with the gas-phase enthalpies reported in Tables 2 and 4; however, the main concern is the nature of the critical points on the PES for these reactions. According to the PCM calculations, reactions 1, 2, 4 and 5 all possess incoming and exiting TSs centered about a stable intermediate. This intermediate lies in a well that is about 2–3-kcal mol^{-1} deep. The reaction barrier ranges from 6.0 to 9.2 kcal mol^{-1} for the cases where the nucleophile attacks a terminal sulfur bearing a hydrogen atom. Attack at the central sulfur of the trisulfide must cross a barrier that is 4.7 kcal mol^{-1} higher than the barrier for attack at the terminal sulfur; therefore, even in solution, there is strong kinetic preference for terminal attack. For these four reactions, the mechanistic pathway remains addition–elimination in solution.

This is in sharp contrast with the PCM results for reactions 3 and 6, where the attack occurs at a terminal sulfur bearing a methyl group. For both of these reactions, the only critical point located on the solvent-phase PES is a TS possessing two S–S distances that are very similar: 2.524 and 2.470 Å in TS-3 and 2.510 and 2.471 Å in TS-6. These TSs are structurally very similar to the intermediates found in their gas-phase analogues; however, these surfaces indicate a concerted reaction whereby the S_{nuc}–S bond is formed as the S–S_{lg} bond is broken or, in other words, an S_N2 reaction.

The mechanism for reactions 3 and 6 is thus dependent on the phase: addition–elimination in the gas phase and S_N2 in water. The difference between these two mechanisms is the presence or absence of an intermediate. In the gas phase, the intermediate is present, but the well may be very shallow: MP2 predicts a well of only 0.1 and 0.7 $kcalmol^{-1}$ for reactions 3 and 6, respectively, while these are somewhat deeper at B3LYP.

We conclude that nucleophilic substitution at sulfur bearing a hydrogen proceeds via an addition–elimination mechanism in both the gas and the solution phase. When the sulfur bears a larger substituent, the mechanism is dependent on the phase. We are continuing to investigate the effect of solution in nucleophilic substitution at sulfur and will report these results in due course.

Acknowledgements. This research was supported by grants from the Robert A. Welch Foundation (W-1442) and the Petroleum Research Fund, administered by the American Chemical Society.

References

1. Lowry TH, Richardson KS (1987) Mechanism and theory in organic chemistry, 3rd edn. Harper and Row, New York
2. Liu T-Y (1977) In: Neurath H, Hill RL, Boeder C-L (eds) The role of sulfur in proteins. Academic, New York, pp 239–402
3. Noiva R, Lennarz WJ (1992) J Biol Chem 267: 3553–3556
4. Nicolaou KC, Dai W-M (1991) Angew Chem Int Ed Engl 30: 1387–1416
5. Whitesides GM, Lilburn JE, Szajewski RP (1977) J Org Chem 42:332
6. Szajewski RP, Whitesides GM (1980) J Am Chem Soc 102: 2011
7. Whitesides GM, Houk J, Patterson MAK (1983) J Org Chem 48: 112–115
8. Singh R, Whitesides GM (1990) J Am Chem Soc 112: 1190–1197
9. Singh R, Whitesides GM (1990) J Am Chem Soc 112: 6304–6309
10. Bachrach SM, Mulhearn DC (1996) J Phys Chem 100: 3535–3540
11. Mulhearn DC, Bachrach SM (1996) J Am Chem Soc 118: 9415–9421
12. Gailbreath BD, Pommerening CA, Bachrach SM, Sunderlin LS (2000) J Phys Chem A 104: 2958–2961
13. Bachrach SM, Hayes JM, Check CE, Sunderlin LS (2001) J Phys Chem A 105: 9595–9597
14. Frisch MJ, Trucks GW, Schlegel HB, Scuseria GE, Robb MA, Cheeseman JR, Zakrzewski VG, Montgomery JA Jr, Stratmann RE, Burant JC, Dapprich S, Millam JM, Daniels AD, Kudin KN, Strain MC, Farkas O, Tomasi J, Barone V, Cossi M, Cammi R, Mennucci B, Pomelli C, Adamo C, Clifford S, Ochterski J, Petersson GA, Ayala PY, Cui Q, Morokuma K, Malick DK, Rabuck AD, Raghavachari K, Foresman JB, Cioslowski J, Ortiz JV, Baboul AG, Stefanov BB, Liu G, Liashenko A, Piskorz P, Komaromi I, Gomperts R, Martin RL, Fox DJ, Keith T, Al-Laham MA, Peng CY, Nanayakkara A, Gonzalez C, Challacombe M, Gill PMW, Johnson B, Chen W, Wong MW, Andres JL, Gonzalez C, Head-Gordon M, Replogle ES, Pople JA (1998) GAUSSIAN 98, revision A.7. Gaussian, Pittsburgh, Pa
15. Becke AD (1993) J Chem Phys 98: 5648–5650
16. Lee C, Yang W, Parr RG (1988) Phys Rev B 37: 785–789
17. Perdew JP (1991) In: Ziesche P, Eschrig H (eds) Unified theory of exchange and correlation beyond the local density approximation. Akademie, Berlin, pp
18. Woon D, Dunning TH Jr (1993) J Chem Phys 98: 1358–1371
19. Dunning TH Jr (1989) J Chem Phys 90: 1007–1023
20. Miertus S, Scrocco E, Tomasi J (1981) Chem Phys 55: 117–129
21. Miertus S, Tomasi J (1982) Chem Phys 65: 239–245
22. Cossi M, Barone V, Cammi R, Tomasi J (1996) Chem Phys Lett 255: 327
23. Pomelli CS, Tomasi J (1997) J Phys Chem A 101: 3561–3568
24. Safi B, Choho K, Geerlings P (2001) J Phys Chem A 105: 591–601
25. Mohamed AA, Jensen F (2001) J Phys Chem A 105: 3259–3268
26. Kona J, Zahradnik P, Fabian WMF (2001) J Org Chem 66: 4998–5007
27. Barone V, Cossi M, Tomasi J (1997) J Chem Phys 107: 3210–3221
28. Reed AE, Weinstock RB, Weinhold F (1985) J Chem Phys 83: 735
29. Pople JA, Scott AP, Wong MW, Radom L (1993) Isr J Chem 33: 345–350
30. Wong MH (1996) Chem Phys Lett 256:391–399
31. Myers AG, Cohen SB, Kwon BM (1994) J Am Chem Soc 116:1255–1271
32. (a) Chandrasekhar J, Smith SF, Jorgenson WL (1984) J Am Chem Soc 106:3049–3050; (b) Chandrasekhar J, Smith SF, Jorgenson WL (1985) J Am Chem Soc 107:154–163; (c) Evanseck JD, Blake JF, Jorgensen WL (1987) J Am Chem Soc 109:2349–2353; (d) Gao J (1991) J Am Chem Soc 113:7796–7797